Chapter 4

DESIGN METHODS FOR CONTROL SYSTEMS

4.1. Controller designs for time delay systems and for slow processes

The dynamics of the process (the plant) can be determined in many industrial control applications from the process response to a step (deterministic) input. Assuming a monotonically changing output process, the simplest parametric models (benchmark type models) are the three or four parameter models with the transfer function (t.f.) in one of the forms

$$P(s)=\frac{k_P}{1+sT}e^{-sT_m}, \tag{4.1.1}$$

$$P(s)=\frac{k_P}{(1+sT)^2}e^{-sT_m}, \tag{4.1.2}$$

$$P(s)=\frac{k_P}{(1+sT_1)(1+sT_2)}e^{-sT_m}, \tag{4.1.3}$$

where: k_P – the process static (DC) gain, T, T_1 and T_2 – the time constants and T_m – the dead time (or the time delay or the transport lag or the latency). The model (4.1.1) will be called first order lag plus dead time (FOLDT) model, and the models (4.1.2) and (4.1.3) will be called second order lag plus dead time (SOLDT) models.

Many design approaches for one-degree-of-freedom (1 DOF) controllers have been developed for these types of benchmark models. The majority of industrial applications with 1 DOF controllers use PI and PID controllers [1]. On the other hand, in certain situations the effect of the dead time can be well compensated by the use of internal model control (IMC) structures; the use of PI and PID controllers is also frequent in this case.

This subchapter presents classical design approaches for the controllers. The design approaches of the 1 DOF controller for processes that can be characterized by the t.f.s in the forms (4.1.1), (4.1.2) and (4.1.3) can be organized as follows from a didactical point of view:

- methods based on previously calculated empirical relations (Ziegler-Nichols, Oppelt, Kopelovich, etc.) based on the control system (CS) structure given in Fig. 4.1.1 (a),
- frequency domain methods based on the CS structure given in Fig. 4.1.1 (a),
- methods applied in the case of IMC structures in the version with Smith predictor based on the CS structure given in Fig. 4.1.1 (b).

The design approaches are mainly focused on tuning methods that offer the computation of the controller parameters. The two basic control structures with 1 DOF controllers are illustrated in Fig. 4.1.1. Some popular design methods for the controllers are presented in [1], [2] and [3].

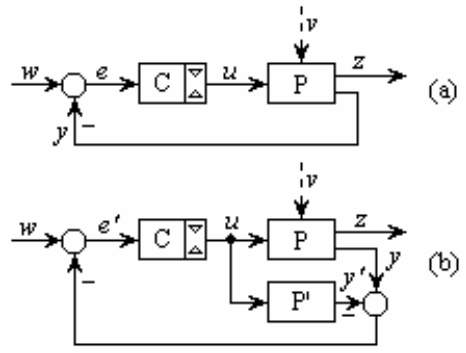

Fig. 4.1.1. Basic control system structures.

A. Tuning Method Based on Reaching the Stability Margin. The advantage of this method is in the fact that it does not require the knowing of the mathematical model (MM) of the process. In turn, it is subjected to constraints concerning the piecewise linearity and the saturation entering of the controller. From a methodical point of view the following operations have to be proceeded:

- the control loop is closed by the use of a proportional controller (with the gain k_R^P) and the plant is determined to reach a steady-state operating point (w_0,y_0) avoiding the external load-type disturbance inputs ($v = 0$);
- the value of k_R^P is increased step by step until the control loop enters a regime characterized by permanent oscillations with the period T_0; the critical value of k_R^P, k_{R0}^P, is highlighted; during the experiment, the designer will display the evolutions of the characteristic variables $\{y, e, u\}$;
- the recommended controller types are chosen accounting for the nature of the plant and the particular features concerning its control;

- the use of the specific relations given by Ziegler and Nichols [2], [3]: the values $\{k_{R0}{}^{P}, T_0\}$ are employed in the computation of the values of the tuning parameters $\{k_R, T_i, T_d\}$ or $\{k_p, k_i, k_d\}$ of the PI or PID controller:

$$C(s) = k_R(1 + \frac{1}{sT_i} + \frac{sT_d}{1+sT_f}), T_f << T_d,$$
$$C(s) = k_p + \frac{k_i}{s} + k_d \frac{s}{1+sT_f}, \tag{4.1.4}$$

  with $k_d = T_d = 0$ for the PI controller;
- the designer will construct the implementation diagram of the controller and he/she will conduct experiments related to the study of the system behavior with respect to the non-simultaneous modifications of reference and disturbance inputs;
- the empirical performance indices, i.e., overshoot (σ_1), settling time (t_s) and natural static coefficient (γ), are used in the assessment of the system quality; these indices are defined in $y(t)$; the evolution of $u(t)$ should be also displayed;
- the behavior of the designed CS (with the tuned parameters) is compared with the behavior of a system with modified controller tuning parameters (sensitivity analysis):

$$k_R = k_{R0} \pm \Delta k_R, T_i = T_{i0} \pm \Delta T_i, T_d = T_{d0} \pm \Delta T_d; \tag{4.1.5}$$

- it is recommented next to design an Anti-Reset-Windup (ARW) measure and to study of the effects of its implementation.

In cases where reaching the stability margin represents a problem, the parameters, which can characterize the critical oscillations, can be calculated analytically.

On the basis of a previous identification of the parameters of the MM in the form (4.1.1), the use of a proportional controller leads to the open-loop t.f. $H_0(s)$:

$$H_0(s) = C(s)P(s) = \frac{k_0}{1+sT} e^{-sT_m},\ k_0 = k_R^P k_P. \tag{4.1.6}$$

The following results are obtained from the frequency domain representation:

$$1 + H_0(j\omega) = 0,\ k_0 e^{-j\omega T_m} + 1 + j\omega T = 0,$$
$$k_0 \cos(\omega T_m) = -1,\ k_0 \cos(\omega T_m) = \omega T. \tag{4.1.7}$$

Equations (4.1.7) permit the determination of the values $\{k_0,\omega\}$ which place the roots of the characteristic equation on the imaginary axis, i.e.,

$$\tan(\omega T_m) = -\omega T,\ k_0^2 = 1 + \omega^2 T^2 . \tag{4.1.8}$$

Introducing the notation $\Omega = \omega T_m$, equation (4.1.8) yields

$$\tan(\Omega) = -(T / T_m)\Omega . \tag{4.1.9}$$

Equation (4.1.9) can be solved relatively easily in a graphical manner giving the solution Ω_0 as shown in Fig. 4.1.2.

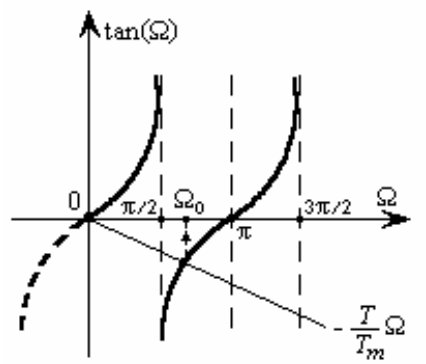

Fig. 4.1.2. Graphical solving of equation (4.1.9).

The controller tuning parameters $\{k_{R0}^{P}, T_0\}$ are next computed:

$$k_{R0}^{P} = (1/k_P)\sqrt{1 + (T/T_m)^2 \Omega_0^2}, T_0 = 2\pi T_m / \Omega_0 . \tag{4.1.10}$$

The above mentioned steps regarding the controller design and implementation will be conducted after the computation of $\{k_{R0}^{P}, T_0\}$. As pointed out in [4], it is of interest to study of the effects of the inexact identification of the parameters $\{k_P, T, T_m\}$.

B. Tuning Method Based on the Relations Due to Oppelt or Chien-Hrones-Reswick. If the process is subjected to open-loop identification by the step response method under the form of the model $P(s)$ given in (4.1.1), one of the following methods is recommended to compute the process parameters:

- the tangent method illustrated in Fig. 4.1.3 (a), where:

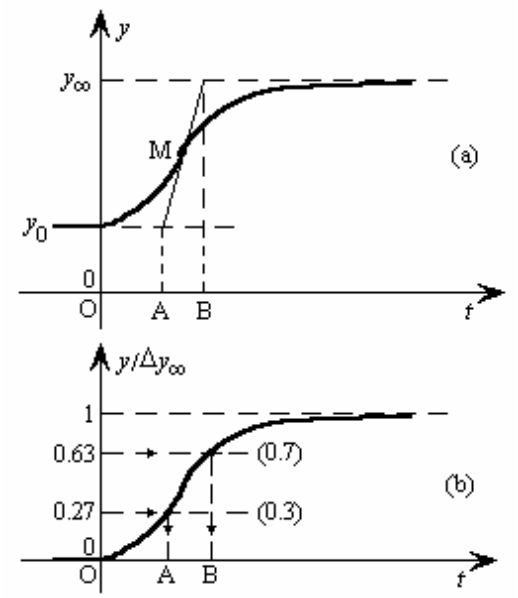

Fig. 4.1.3. Computation of process parameters.

$$k_P = \Delta y_\infty / \Delta u_\infty,\ T = \overline{\mathrm{OA}},\ T_m = \overline{\mathrm{AB}}; \tag{4.1.11}$$

- the method given by Cohen-Coon or by other authors, illustrated in Fig. 3 (b), where:

$$\begin{aligned} k_P &= \Delta y_\infty / \Delta u_\infty,\ T = 1.5(\overline{\mathrm{OB}} - \overline{\mathrm{OA}}), \\ T_m &= 1.5(\overline{\mathrm{OA}} - \overline{\mathrm{OB}}/3), \end{aligned} \tag{4.1.12}$$

or

$$\begin{aligned} k_P &= \Delta y_\infty / \Delta u_\infty,\ T = 1.25(\overline{\mathrm{OB}} - \overline{\mathrm{OA}}), \\ T_m &= 1.5(\overline{\mathrm{OA}} - \overline{\mathrm{OB}}/3). \end{aligned} \tag{4.1.13}$$

The relations grouped in tables given by Oppelt, Chien-Hrones-Reswick, Cohen-Coon, etc. [2], are next used in the controller tuning.

C. Strejc's Method. This method has the specific feature that in some certain conditions the MM of the plant is in the form (4.1.2) or (4.1.3), where the dead time T_m is a real one or a computational one. The controller design methods are various and often dedicated to some classes of applications [5], [6].

D. Using the Smith Predictor. The study and implementation of the control structures based on Smith predictor (Fig. 4.1.1 (b)) have an advantage in the simultaneous treatment of the idea of IMC and of the prediction based on the anticipation effect. The MM of the plant is separated in its two components, the rational part and the component that characterizes the dead time:

$$P(s) = P^{'}(s)e^{-sT_m}. \tag{4.1.14}$$

This enables the separate design of the controller $C(s)$ relative to the part $P^{'}(s)$. Two controller tuning methods can be applied:

- the analytical design in the frequency domain;
- the design based on the application of the Modulus Optimum method or of the Extended Symmetrical Optimum method [7] in its particular version adapted to the plants without integral component [8].

The following computational steps are applied in the first method:

- the experimental identification by the step response method (k_P, T, T_m) in different operating conditions;
- the acceptance of the control solution based on the PI controller with the t.f.

$$C(s) = \frac{k_c}{s}(1 + sT_c); \tag{4.1.15}$$

- the determination of the frequency response function and of its magnitude and phase functions:

$$|H_0(j\omega)| = (k_c k_P / \omega)\sqrt{\frac{1+(\omega T_c)^2}{1+(\omega T)^2}},$$
$$\arg H_0(j\omega) = \pi/2 + \tan^{-1}(\omega T_c) - \tan^{-1}(\omega T); \tag{4.1.16}$$

- the imposing of a desired phase margin, $\varphi_{md} \in [\pi/4, \pi/3]$ and the calculation of the crossover frequency ω_c;
- the calculation of the tuning parameters $\{k_c, T_c\}$; the solution is not unique, and this offers a large variety of case studies with appropriate analyses;
- the calculation of the feedback compensator, with the t.f. $C_C(s)$, using the first-order Pade approximation:

$$e^{-sT_m} \approx \frac{1 - sT_m/2}{1 + sT_m/2},\ C_C(s) = \frac{k_P}{1+sT} \cdot \frac{sT_m}{1 + sT_m/2}; \tag{4.1.17}$$

- the implementation of the solution on the real-world process and the effectuation of real-time experiments in several operating conditions in order to validate the solution.

Application 4.1.1: The equipment "Air Stream and Temperature Control Plant" (ASTCP, Fig. 4.1.4) represents a multifunctional product of Amira GmbH [9], which can ensure the control of two parameters, the air temperature and the air stream. The functional block diagram of the ASTCP equipment is illustrated in Fig. 4.1.5. The strictly speaking plant is characterized by:

- two input variables: the ventilator motor speed and the control signal of the heating element;
- five measurable variables: the air stream, the air temperature (in two points), the air pressure and the position of the air admission throttle.

In this context, the equipment permits the construction of numerous control structures for temperature, stream and pressure control. The application presented as follows is described in [4], and it deals with the temperature control in the measuring point 2 (probe 2) where the operating conditions are modified.

Fig. 4.1.4. Laboratory equipment ASTCP in the Intelligent Control Systems Laboratory of the Politehnica University of Timisoara, Romania.

The plant identification (actuators, strictly speaking plant and measuring elements) under the form of the t.f. (4.1.1) is performed for different initial and final values of the temperature (T_{10} and T_{20}) and in different initial operating situations. The plant static gain k_P can be determined:

- by experimental approximation (the usual way) or
- by the use of the least-squares method based on Matlab programs.

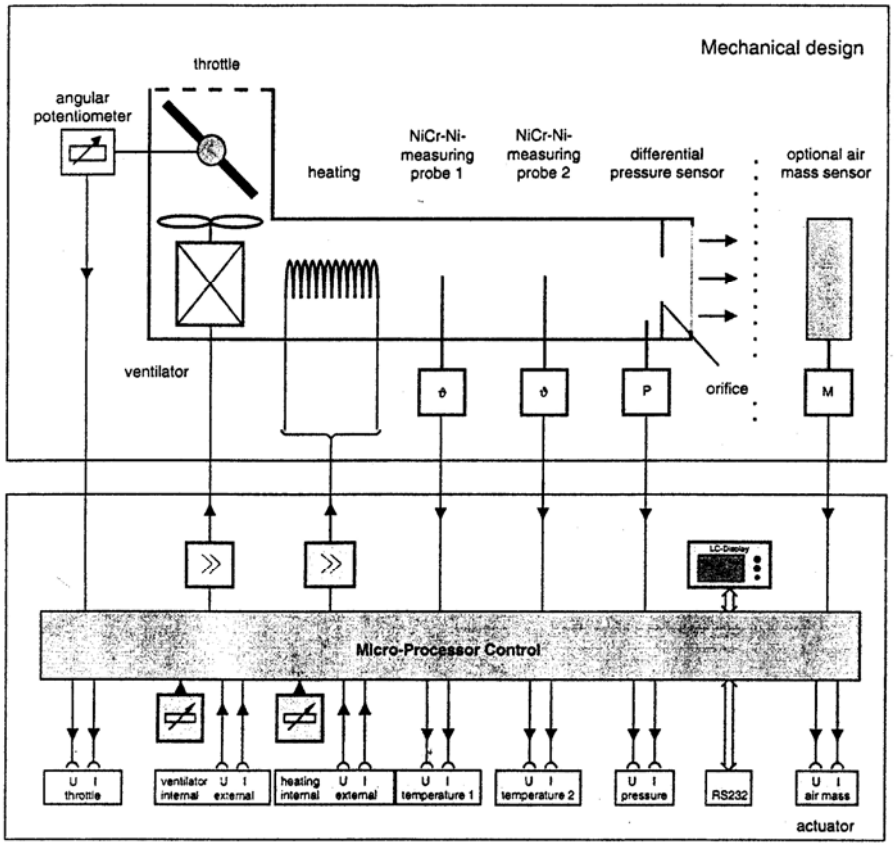

Fig. 4.1.5. Functional block diagram of laboratory equipment ASTCP [9].

For the large variety of possible situations, the plant static gain k_P varies within large limits (0.5 … 1.2) which ensures many possible sets of controller parameters, Fig. 4.1.6 illustrates the dynamic response of the plant with respect to a step variation of the heating degree with 30% in the following initial conditions: 45% opening of air admission, heating degree 50 % and ventilator motor speed 50 %. The plant identification leads to the plant parameter values $k_P \approx 0.93$, $T \approx 2.4$ s, $T_m \approx 0.93$ s. The controller design and tuning can be done on the basis of these results.

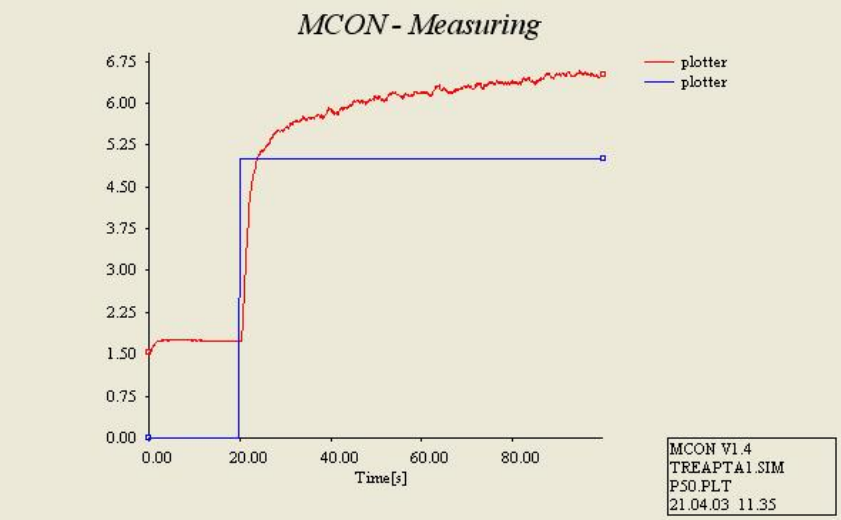

Fig. 4.1.6. Control system behavior (controlled output and control signal versus time) in the case of using the PI controller [4].

The use of a PI controller with the parameters tuned in terms of the Ziegler-Nichols relations with the parameters defined in the t.f. (4.1.4) with $k_d = 0$ leads to the following values of these parameters: $k_p = 1.92$, $k_i = 0.83$. The block diagram of the control system with the PI controller implementation in MCON (described in [9]) is presented in Fig. 4.17. The variation of the control signal and the control system response (with PI controller) with respect to the step modification of the reference input followed by a step modification of the disturbance input (the ventilator motor speed) are illustrated in Fig. 4.1.8.

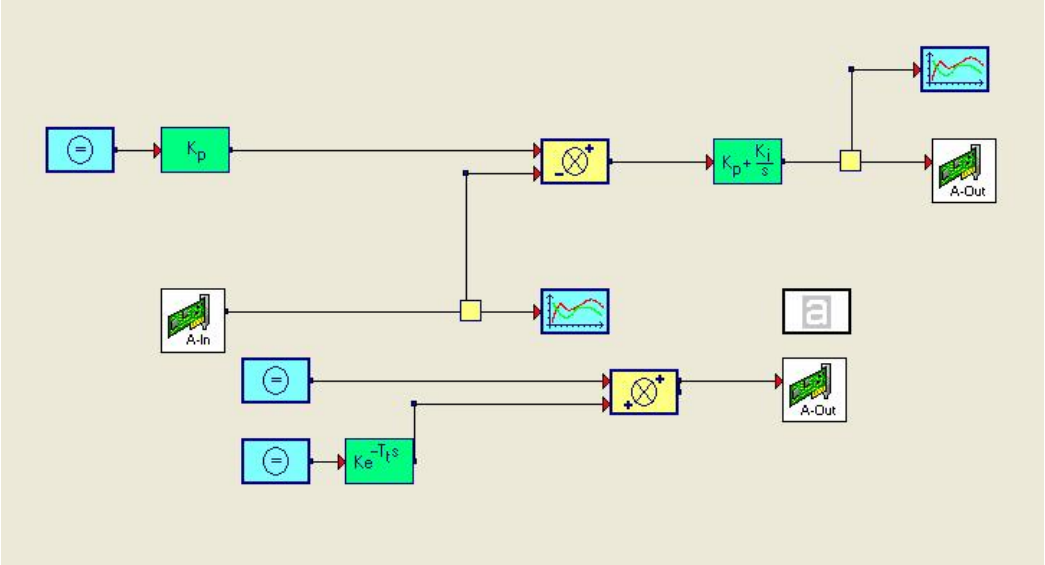

Fig. 4.1.7. Block diagram of control system implemented with PI controller [4].

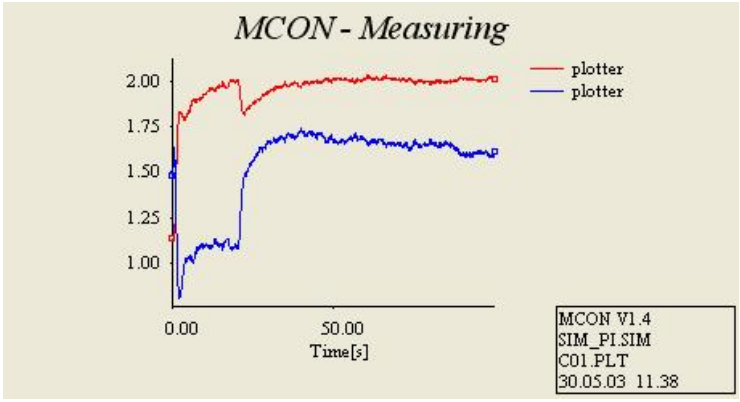

Fig. 4.1.8. Control system behavior (controlled output and control signal versus time) in the case of using the PI controller [4].

The second control structure concerns a Smith predictor together with a PI controller tuned in the frequency domain and implemented according to Fig. 4.1.9. The experimental conditions were identical to those presented in the previous case. The control system response in this case is illustrated in Fig. 4.1.10.

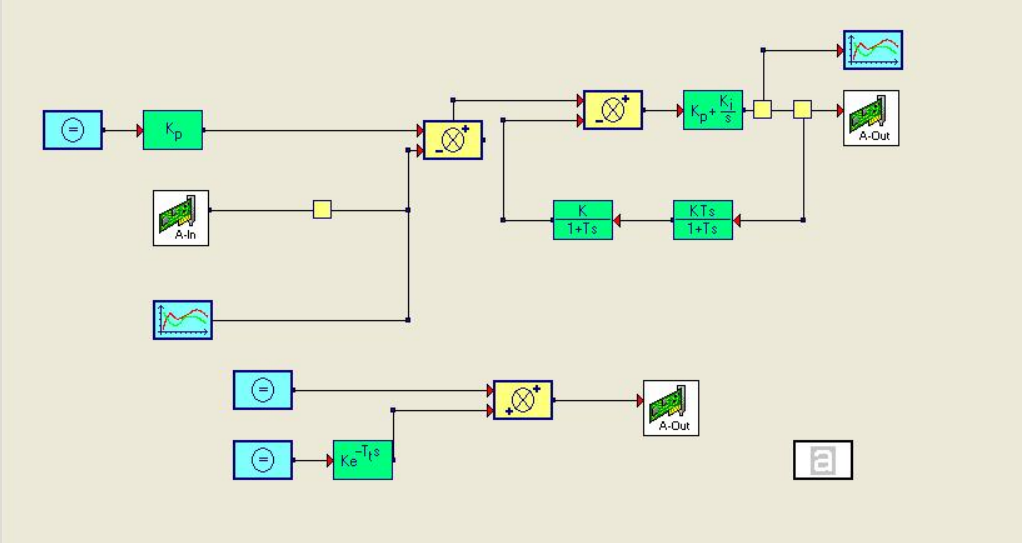

Fig. 4.1.9. Block diagram of control system implemented with Smith predictor and PI controller [4].

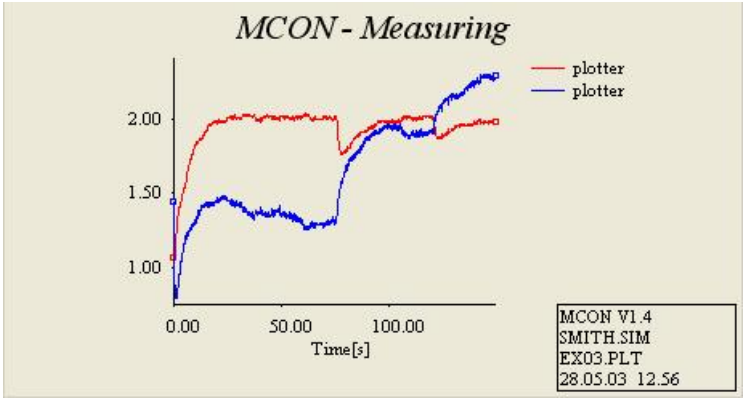

Fig. 4.1.10. Control system behavior (controlled output and control signal versus time) in the case of using the Smith predictor and the PI controller [4].

4.2. Modulus Optimum method and Symmetrical Optimum method

Kessler has elaborated in 1958 the basic version of the Symmetrical Optimum (SO) method, and it is characterized by the fact that in the open-loop t.f. $H_0(s)$:

$$H_0(s) = H_C(s)H_P(s), \tag{4.2.1}$$

with $H_C(s)$ – the controller t.f. and $H_P(s)$ – the controlled plant t.f., leads to a double pole in the origin. This can correspond to various situations:

- the plant is characterized by an integral component and the controller brings the second one in order to ensure the condition of zero steady-state control error and zero static coefficient,
- the plant does not contain any integral component, but the requirement for zero control error with respect to the ramp modification of the reference input leads to the necessity that the controller should bring the two integral components, and others.

This subchapter will discuss the following topics:

- a short overview on Kessler's version of the SO method (both in the time domain and in the operational domain);
- an application of the SO method to some low order benchmarks given in [1];
- extensions of the SO method;
- applications.

The tuning methods presented in this subchapter are applied mainly to fast processes (plants). The efficiency of controller tuning in terms of the SO method can be proved both in the time domain and in the frequency domain as well [3].

4.2.1. A short overview on the Symmetrical Optimum method

The basic version of the SO method [10] accepts that the controlled plant has its t.f. expressed as

$$H_P(s) = \frac{k_P}{(1+sT_\Sigma)\prod_{\nu=1}^{n}(1+sT_\nu)}, \tag{4.2.2}$$

or in the case of an included integral component:

$$H_P(s) = \frac{k_P}{s(1+sT_\Sigma)\prod_{\nu=1}^{n}(1+sT_\nu)}, \tag{4.2.3}$$

where T_Σ includes the effects of the small time constants of controlled plant, and T_ν represent the large time constants of the plant ($\nu = 1 \ldots n$).

It is well accepted that the quality of the system transients is determined by the shape of the open-loop frequency plots, $H_0(j\omega)$ in the zone of the crossover frequency ω_c. For ensuring proper control system performance (σ_1 – overshoot, t_s – settling time, t_1 – 0-to-100% rise time, etc.) it is required that the value of ω_c should be as large as possible representing an acceptable value for the phase margin (reserve), φ_r.

For the large time constants of the controlled plant T_ν, the t.f. (4.2.2) – transferred into the frequency domain – for large values of the frequency ω the following approximation will be accepted:

$$1 + j\omega T_\nu \approx j\omega T_\nu . \tag{4.2.4}$$

Therefore, (4.2.2) will be approximated by

$$H_P(s) \approx \frac{k_P}{(1+sT_\Sigma)\prod_{\nu=1}^{n}(sT_\nu)} . \tag{4.2.5}$$

Using a typical controller (PI, PID, etc.) with the theoretical t.f.

$$H_C(s) = \frac{\prod_{\mu=1}^{m}(1+s\tau_\mu)}{\tau s} \tag{4.2.6}$$

the open-loop t.f. (4.2.1) obtains the form

$$H_0(s) \approx \frac{k_P\prod_{\mu=1}^{m}(1+s\tau_\mu)}{\tau s\,(1+sT_\Sigma)\prod_{\nu=1}^{n}(sT_\nu)} . \tag{4.2.7}$$

Performing some computations in (4.2.7), assuming the condition m = n, it can be expressed as the equivalent form [11]

$$H_0(s) \approx \frac{\prod_{\nu=1}^{n}(1+s\tau_\nu)}{\tau_e\, s\,(1+sT_\Sigma)\prod_{\mu=1}^{n}(s\tau_\mu)}, \tag{4.2.8}$$

where

$$\tau_e = \frac{\tau}{k_P}\cdot\frac{\prod_{\nu=1}^{n}T_\nu}{\prod_{\mu=1}^{n}\tau_\mu}. \tag{4.2.9}$$

In Kessler's version the proper control system behavior is accomplished if the following three requirements are fulfilled [10]:

- the congruence of the time constants brought by the controller:

$$\tau_1 = \tau_2 = \ldots = \tau_m = \tau_c; \tag{4.2.10}$$

- a first optimum condition:

$$\tau_c = 4\,n\,T_\Sigma; \tag{4.2.11}$$

- a second optimum condition:

$$\tau_e = 2\,T_\Sigma. \tag{4.2.12}$$

The following combined restricted condition will result from (4.2.11) and (4.2.12):

$$\tau_c = 2\,n\,\tau_e. \tag{4.2.13}$$

The substitution of the conditions (4.1.10) in (4.2.8) leads to

$$H_0(s) \approx \frac{(1+\tau_c s)^n}{(1+sT_\Sigma)(\tau_c s)^n\,\tau_e s} = \frac{[1+1/(s\tau_c)]^n}{\tau_e\, s(1+sT_\Sigma)}. \tag{4.2.14}$$

If in the expression of the nominator there are used only the first two terms of the binomial formula in terms of (4.2.11) and (4.2.12), it will result that the open-loop t.f. (4.2.14) will obtain the practical useful form [1]

$$H_0(s) \approx \frac{1+4T_\Sigma s}{8T_\Sigma^2 s^2(1+T_\Sigma s)}. \tag{4.2.15}$$

Accordingly, the closed-loop t.f. with respect to the reference input *w* can be expressed as

$$H_w(s)=\frac{b_0+b_1 s}{a_0+a_1 s+a_2 s^2+a_3 s^3}, \tag{4.2.16}$$

with $a_0= b_0= 1$, $a_1= b_1= 4T_\Sigma$, $a_2= 8T_\Sigma^2$, $a_3= 8T_\Sigma^3$, or, in a factorized version:

$$H_w(s)=\frac{1+4T_\Sigma s}{(1+2T_\Sigma s)(1+2T_\Sigma s+4T_\Sigma^2 s^2)}. \tag{4.2.17}$$

However, the obtained dynamic control system performance indices $\sigma_1\approx$ 43%, $t_s\approx 16.5T_\Sigma$, $t_1\approx 3.1T_\Sigma$, are seldom acceptable and require the improvement. Referring the t.f. (4.2.17), this is usually done in the input-output framework by pre-filtering the reference input with filters that suppress the effect of either only the zero ($-1/4T_\Sigma$) or the pair of complex conjugated poles (pole-zero cancellation, control based on an inverse model of the system).

The main **drawback** of the SO method is the relatively small phase margin of the control loop, $\varphi_r \approx 36^o$. That is reflected in the increased sensitivity with respect to parametric modifications.

As mentioned in [11], some papers (for example, [12]) consider that this method belongs to both Kessler and Naslin.

4.2.2. A practical version of the Symmetrical Optimum method

Starting with the form (4.2.16) of the closed-loop t.f. $H_w(s)$, Åström and Hägglund have considered in [1] that the fulfillment of the conditions

$$2a_0a_2=a_1^2,\ 2a_1a_3=a_2^2 \tag{4.2.18}$$

ensures for the t.f. (4.2.16) optimal performance guaranteed by the SO method and it offers, by design, a compact manner for computing the controller tuning parameters. Many remarkable applications are related to the field of electrical drives, characterized by t.f.s expressed as benchmark type plants:

$$H_P(s)=\frac{k_P}{s(1+sT_\Sigma)} \tag{4.2.19}$$

or

$$H_P(s)=\frac{k_P}{s(1+sT_\Sigma)(1+sT_1)}, \tag{4.2.20}$$

where $T_1 >> T_\Sigma$ is the large time constant of the plant.

The use of a PI or of a PID controller having the t.f. (4.2.21) and (4.2.22), respectively:

$$H_C(s)=\frac{k_c}{s}(1+sT_c)\,, \tag{4.2.21}$$

$$H_C(s)=\frac{k_c}{s}(1+sT_c)(1+sT_c')\,, \tag{4.2.22}$$

with $T_c' = T_1$ (pole-zero cancellation), simplifies enough the design steps.

The application of the optimization relations (4.2.18) leads to the t.f.s $H_0(s)$ and $H_w(s)$ under the forms (4.2.15) and (4.2.17), respectively.

The Bode plots of the optimal transfer function $H_0(s)$ given in (4.2.15) is symmetrical around the crossover frequency $\omega_c = 1/(2T_\Sigma)$. That is the main motivation for the name Symmetrical Optimum in terms of Åström and Hägglund [1].

The parameters of the PI controllers and of the PID controllers are computed by means of the compact relations

$$k_c=\frac{1}{8k_P T_\Sigma^2},\ T_c=4T_\Sigma\ \ (T_c'=T_1)\,. \tag{4.2.23}$$

The justification pointed out in [1] makes the presentation of the SO method close to the Modulus Optimum method.

Requirements close to those given by the SO method have been formulated also by many other papers as, for example, [8], [13] and [14]; each of the contributors points out interesting particular aspects.

4.2.3. Extensions of the Symmetrical Optimum method

The "optimal performance" guaranteed by the SO method – namely, $\sigma_1 \approx 43\%$ (overshoot), $t_s \approx 16.5T_\Sigma$ (settling time), $t_1 \approx 3.1T_\Sigma$ (0-to-100% rise time) and a small phase margin, $\varphi_r \approx 36^0$ (the main drawback of the SO method) – are seldom acceptable, so the retuning of the controller parameters or the use of adequate designed reference filters are strongly recommended. Efficient ways for performance enhancement are based on two extensions of the SO-m, **the Extended Form of the Symmetrical Optimum Method** (the ESO method), and **the Double Parameterization of the Symmetrical Optimum Method** (the 2p-SO method). Both methods (presented in [7], [15] and [16]) are based on a generalized form of equations (4.2.18) expressed as

$$\sqrt{\beta}\, a_0\, a_2 = a_1^2,\ \sqrt{\beta}\, a_1\, a_3 = a_2^2, \tag{4.2.24}$$

where β is the design parameter. These two methods are focused to fulfill an increased value for the phase margin, good (better) tracking performances and efficient disturbance rejection.

A. The Extended Symmetrical Optimum method (**the ESO method**) [3]. The ESO method is dedicated mainly to positioning systems with processes characterized by the t.f.s with an integral (I) component given (4.2.19) and (4.2.20). Applying the optimization relations (4.2.24) leads to the characteristic t.f.s $H_0(s)$ (open-loop t.f.) and $H_r(s)$ (closed-loop t.f. with respect to the reference input with the notation *r* or *w*)

$$\begin{aligned} H_0(s) &= \frac{1+\beta T_\Sigma s}{\beta\sqrt{\beta}\, T_\Sigma^2 s^2 (1+T_\Sigma s)}, \\ H_r(s) &= H_w(s) = \frac{1+\beta T_\Sigma s}{\beta\sqrt{\beta}\, T_\Sigma^3 s^3 + \beta\sqrt{\beta}\, T_\Sigma^2 s^2 + \beta T_\Sigma s + 1}. \end{aligned} \tag{4.2.25}$$

The ESO method ensures the compact design relations for the parameters, in the general form

$$k_c = \frac{1}{k_P\, \beta\sqrt{\beta}\, T_\Sigma^2},\ T_c = \beta T_\Sigma\ \ (T_c' = T_1), \tag{4.2.26}$$

which leads to significantly improved performance. Fig. 4.2.1 illustrated the main CS performance indices as function of the design parameter β.

The ESO method also offers a good support in controller design for plants with variable parameters (for example, in application characterized by the variation of k_P within the domain [k_{Pmin}, k_{Pmax}] and similarly for T_Σ) and the possibility for online computing the value of β which ensures a minimum guaranteed phase margin. This is the situation imposed by electrical drives with Variable Moment of Inertia (VMI). The recommended domain for β, also pointed out in Fig. 4.2.1, is $4 < \beta \le 9\,(16)$.

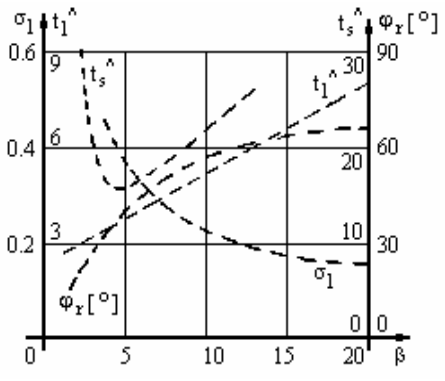

Fig. 4.2.1. Performance indices σ_1, $t_s^{\wedge} = t_s / T_\Sigma$, $t_1^{\wedge} = t_1 / T_\Sigma$ *and* $\varphi_r\,[^\circ]$ *versus* β.

Useful connections of the results with those obtained by minimizing the integral quadratic performance indices are proved in [17]. Several analyses are presented in [18], and a part of them will be overviewed as follows. Some representative recent generalizations to fuzzy control systems and to neuro-fuzzy control systems with applications in electrical drives with VMI are given in [19]–[23].

B. The double parameterization of the SO method (**the 2p-SO method**). The 2p-SO method introduced in [8] and [15] is dedicated to driving systems (speed control, characterized by t.f.s without an I component:

$$P(s) = \frac{k_P}{(1+sT_\Sigma)(1+sT_1)} \quad \text{(a)},$$
$$P(s) = \frac{k_P}{(1+sT_\Sigma)(1+sT_1)(1+sT_2)} \quad \text{(b)}, \tag{4.2.27}$$

with $T_1 > T_2 >> T_\Sigma$. The 2p-SO method is based on the generalized optimization conditions (4.2.24) and on a supplementary defined parameter *m*:

$$m = T_\Sigma / T_1 \quad (T_\Sigma / T_1 << 1). \tag{4.2.28}$$

The characteristic t.f.s $H_0(s)$ and $H_r(s)$ will finally obtain the optimized forms given in (4.2.29) and in (4.2.30), respectively:

$$H_{0opt}(s)=\frac{1+\beta T_{\Sigma m}s}{\beta\sqrt{\beta}\,T_{\Sigma}^{'}\dfrac{m}{(1+m)^2}s(1+sT_1)(1+sT_{\Sigma})}, \tag{4.2.29}$$

$$\begin{aligned} H_{r\,opt}(s)&=\frac{(1+\beta T_{\Sigma m}s)}{\beta\sqrt{\beta}\,T_{\Sigma}^{'3}s^3+\beta\sqrt{\beta}\,T_{\Sigma}^{'2}s^2+\beta T_{\Sigma}^{'}s+1}\\ &=\frac{(1+\beta T_{\Sigma m}s)}{(1+\sqrt{\beta}\,T_{\Sigma}^{'}s)[1+(\beta-\sqrt{\beta})T_{\Sigma}^{'}s+\beta T_{\Sigma}^{'2}s^2]}, \end{aligned} \tag{4.2.30}$$

with $T_{\Sigma}^{'}=\dfrac{T_{\Sigma}}{(1+m)}$. The compact design relations in this case are

$$k_c=\frac{(1+m)^2}{\beta\sqrt{\beta}\,k_P T_{\Sigma}m}(1+m),\ T_c=\beta T_{\Sigma}\frac{[1+(2-\sqrt{\beta})m+m^2]}{(1+m)^3}. \tag{4.2.31}$$

The 2p-SO method mainly ensures the efficient disturbance rejection for a special case of servo-system applications with "great and variable" moment of inertia. The CS performance indices regarding the reference input are synthesized in Fig. 4.2.2. Extended and useful conclusions are presented in [16].

Compared to other classical benchmark-type model oriented tuning methods [1], the 2p-SO method can be recommended for servo systems (speed control) characterized with great differences between the large and the small time constants ($0.05<m\le 0.2$) and high performance imposed regarding load disturbances. Comparing the control system performance with that ensured by the Modulus Optimum method (the MO method), (β in the of domain of $4<\beta\le 9\,(12)$) the effect of load disturbances is faster rejected. The method is easily applicable to the online retuning of the controller parameters.

The digital quasi-continuous (QC) implementation of the PI(D) controller as digital control algorithm can be supported by the informational diagram presented in Fig. 4.2.3. The additional state variable x_k is associated to the I component, and an ARW measure is inserted. The equivalency between the parameters {K_{pid}, K_i, K_d, K_{arw}} and the continuous parameters of the controllers {k_r, T_r, T_r'} is easily calculable, and it depends on the sampling period value, $T_s=T_e$. If the controllers are developed on the basis of linearized models, the solution allows the bumpless switching from one controller to another one depending on the operating points [24].

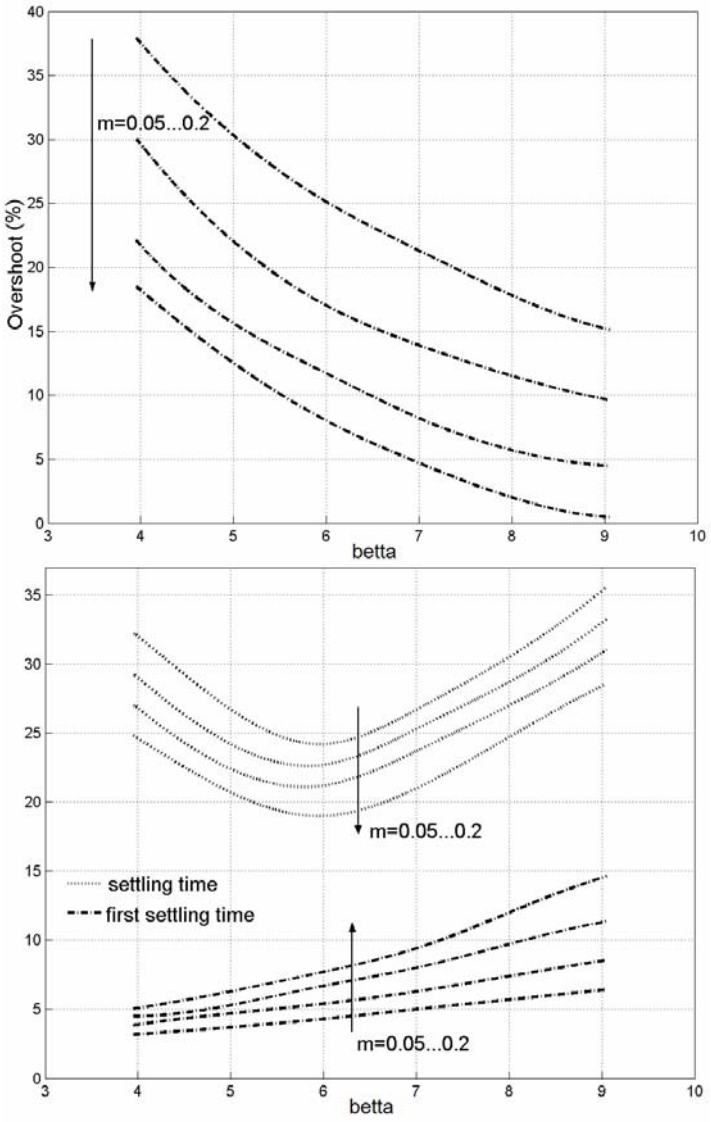

Fig. 4.2.2. CS performance regarding the reference input: $\sigma_{1,r}, t_{s,r}, t_{1,r} = f(\beta)$, *with m – parameter.*

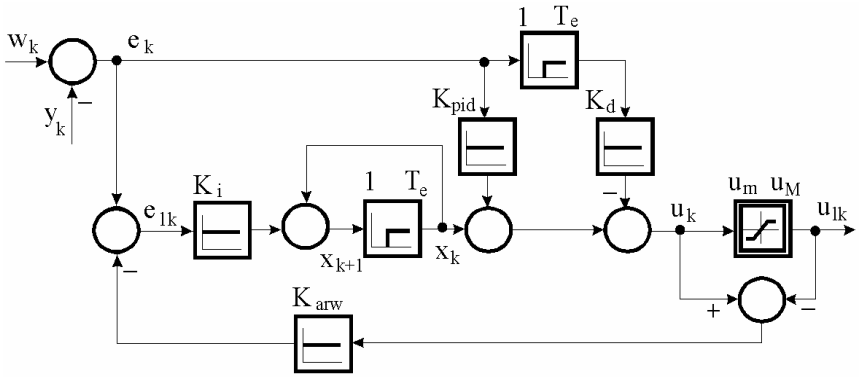

Fig. 4.2.3. A quasi-continuously operating PID digital control algorithm implementation.

C. Sensitivity analysis in the frequency domain. The CS performance indices versus β can be represented in a graphical form in the frequency domain. An efficient measure of the sensitivity and of the robustness of our extensions is based on the relation of the sensitivity function $S_0(s)$ and of the complementary sensitivity function $T_0(s)$, the Nyquist plots and the $M_{S0} = f(\beta)$ circles, and the values of M_{S0}^{-1} versus β (in Fig. 4.2.4), the phase margin φ_r versus β and/or Bode diagrams for different values of β and *m*.

For example, Fig. 4.2.4 illustrates the Nyquist curves, the $M_{S0} = f(\beta)$ circles and the $M_{S0}^{-1} = f(\beta)$ circles for the ESO method considering the representative values of β, $\beta \in \{4,9,16\}$. Detailed diagrams and discussions are offered in [16] for the 2p-SO method.

Fig. 4.2.5 illustrates these diagrams just for the extreme situation characterized by $m = 0.05$ and $\beta \in \{4, 9, 12\ (20)\}$. The curves point out the increase of robustness when the value of β is increased. Such diagrams can be useful for the computer-aided controller design by allowing to set the value of β according to the performance specifications.

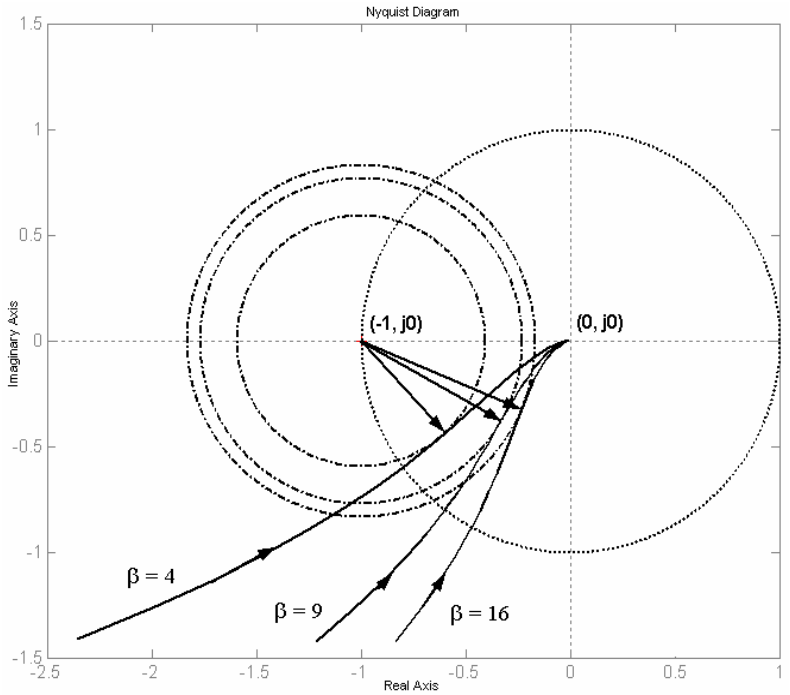

Fig. 4.2.4. Nyquist curves and M_{S0}^{-1} *circles for* $\beta \in \{4,9,16\}$ *in the case of the ESO method.*

D. Further performance enhancement. Alternative controller structures. Both extensions found applications incorporated in alternative control structures and algorithms. Such applications are exemplified as follows. Starting with Fig. 4.2.6, a particular case of control structure (CS) containing controllers with non-homogenous dynamics with respect to the two inputs is presented in Fig. 4.2.7 [24].

The controller blocks are characterized by their own t.f.s. Starting with the CS with 1 DOF controller given in Fig. 4.2.7 (a), the use of the reference filter $F_r(s)$ can ensure an efficient pole-zero compensation. This approach allows a two-degree-of-freedom (2 DOF) interpretation of the design [25].

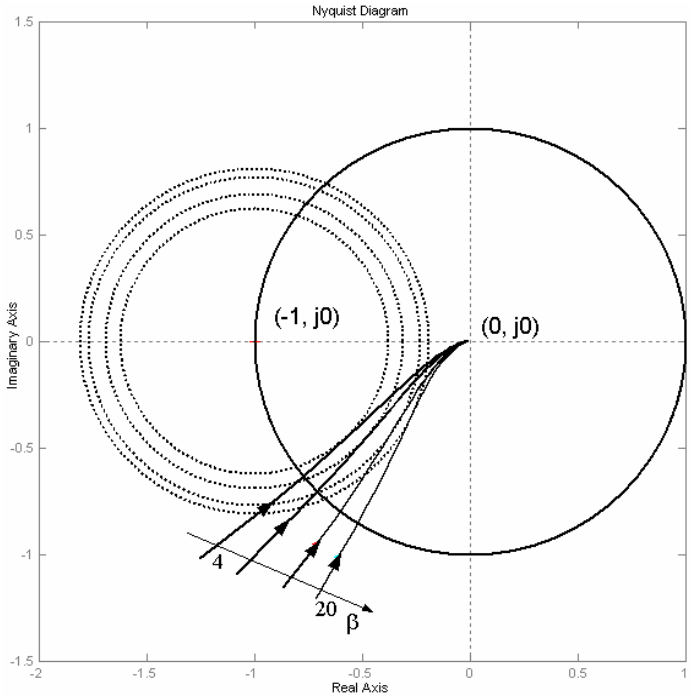

Fig. 4.2.5. Nyquist curves and M_{S0}^{-1} *circles for* $m = 0.05$ *and* $\beta \in \{4,9,12\ (20)\}$ *in case of the 2p-SO method.*

The performance enhancement is exemplified here only for the ESO method [11]. The same methodology is applied for the 2p-SO method [16].

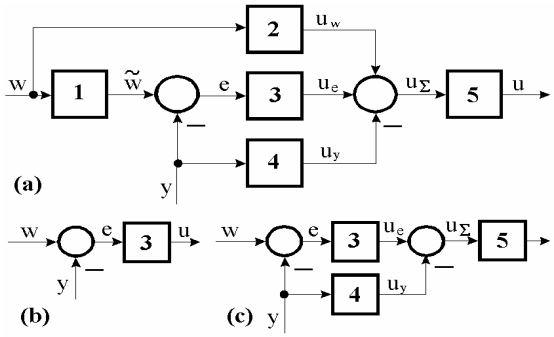

Fig. 4.2.6. Typical controller structures and particular forms of the modules [24].

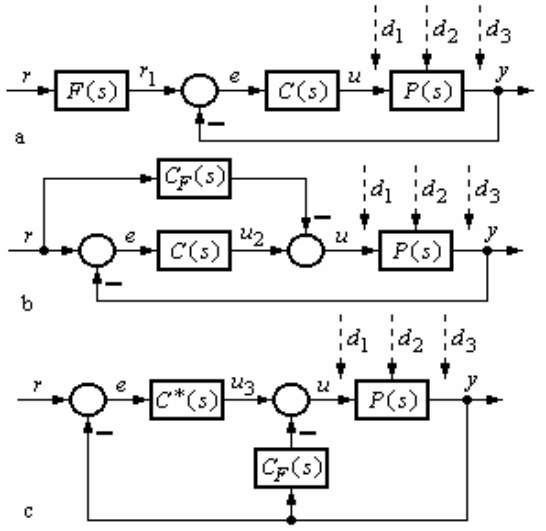

Fig. 4.2.7. Structures of 1 DOF and of 2 DOF controllers as extensions of 1 DOF controller.

A first version of reference filter $F_r(s)$ is recommended to compensate for the effect of the complex conjugated poles in (4.2.25) (also in (4.2.30) and, together with this, the effect of the zero:

$$F_r(s)=\frac{1+(\beta-\sqrt{\beta})T_\Sigma s+\beta T_\Sigma{}^2 s^2}{(1+\beta T_\Sigma s)(1+T_f s)}. \tag{4.2.32}$$

Consequently, the control system behavior in the relation $r\to r_1\to y$ becomes aperiodic, with the main performance indices $\sigma_1=0$ and $t_s\approx(3...5)(\beta-1)T_\Sigma$ (and φ_r according to Fig. 4.2.1):

$$\widetilde{H}_r(s)=\frac{1}{(1+\beta T_\Sigma s)(1+T_f s)}. \tag{4.2.33}$$

A second version of filter can be used to compensate only for the effect of the zero in (4.2.30). This results in the filter t.f.

$$F_r(s)=\frac{1}{1+\beta T_\Sigma s}. \tag{4.2.34}$$

The control system behavior in the relation $r \to r_1 \to y$ is given by the following t.f. and the closed-loop system has an oscillatory behavior only for $\beta < 9$:

$$\widetilde{H}_r(s) = \frac{1}{(1+\sqrt{\beta}\,T_\Sigma s)[1+(\beta-\sqrt{\beta})T_\Sigma s+\beta\,T_\Sigma^2 s^2]}. \tag{4.2.35}$$

Similar types of filters are used in the case of the 2p-SO method having β and m as parameters [16].

E. Equivalency between 1 DOF (PID) and 2 DOF controllers. Let us consider the block diagram given in Fig. 4.2.7 (a). Replacing the feedback controller $C(s)$ on the input channel and the forward loop, this CS can be transposed into a 2 DOF CS in its classical RST representation, where $R(\ )$, $S(\ )$ and $T(\ )$ are the specific polynomials [26].

The PI or PID controllers (with/without reference filters) can be restructured in form of the 2 DOF controller, and vice-versa, where the presence of a conventional controller can be highlighted. Two types of such rearranged PI(D) structure are detailed in Fig. 4.2.7 (b) and (c). The rearrangements allow take into account the design experience from case of PI and PID controllers.

For example, if the controller from Fig. 4.2.7 (b) is be characterized by a continuous t.f. with the "traditional" [1] tuning parameters $\{k_R,\ T_i,\ T_d,\ T_f\}$. The t.f.s of the equivalent blocks are

$$\begin{aligned} C(s) &= \frac{u(s)}{e(s)} = k_R\left(1+\frac{1}{sT_i}+\frac{sT_d}{1+sT_f}\right), \\ C_F(s) &= \frac{u_f(s)}{r(s)} = k_R\left(\alpha_1+\alpha_2\frac{sT_d}{1+sT_f}\right). \end{aligned} \tag{4.2.36}$$

For the CS given in Fig. 4.2.7 (c) (with the notation $C(s) = C^*(s)$) the t.f.s are

$$\begin{aligned} C^*(s) &= \frac{u(s)}{e(s)} = k_R\left[(1-\alpha_1)+\frac{1}{sT_i}+(1-\alpha_2)\frac{sT_d}{1+sT_f}\right], \\ C_P(s) &= \frac{u_f(s)}{r(s)} = k_R\left(\alpha_1+\alpha_2\frac{sT_d}{1+sT_f}\right). \end{aligned} \tag{4.2.37}$$

The connections of these blocks are illustrated in Table 4.2.1 which depends on the values of α_1 and α_2 (parameters). The choice of a certain representation of the controller depends on:

- the structure of the available controller;
- the adopted algorithmic design method and the result of this design.

Table 4.2.1. Connections between 2-DOF controller and extended 1-DOF controller structure (P – proportional, D – derivative, I – integral, L1(2) – first (second) order lag filter) [18].

Fig. 4.2.7 (a)		F(s)	-	F(s)C(s)	C(s)	Remarks
Fig. 4.2.7 (b)		-	C_F	C(s)–C_F(s)	C(s)	-
Fig. 4.2.7 (c)		-	C_P	C*(s)	C*(s)+C_P(s)	-
α_1	α_2	-	-	(ref. channel)	(feedback)	
0	0	1	0	PID	PID	1-DOF controller
0	1	PDL2	DL1	PI	PID	1-DOF with non-homogenous behavior
1	0	PD2L2	P	PID-L1	PID	
1	1	PL2	PDL2	I	PID	
α_1	α_2	PID controller with pre-filtering (2-DOF controller)				

The comparisons between the 2 DOF CS and the 1 DOF CS can be carried out on the basis of the Cs structures presented in Fig. 4.2.7. Some results in this context are presented in [16] and [26].

Application 4.2.1: Let us consider the representative controlled plants (processes) in the field of electrical drives exemplified by the Direct Current (DC) motors (DC-ms) and by Brushless Direct Current (BLDC) motors (BLDC-ms) with an internal control loop. The ESO method will be applied as follows to design the controller in the outer control loop (the speed control loop) in a cascade control system structure.

In the symmetrical operating mode [27], the mathematical models of BLDC-m and DC-m are very close. This aspect leads to similarities in the controller design and to cost-effective implementations. In case of BLDC-m based drives the current switching is obtained by specialized converters with commutation time determined by the position of the rotor. The block diagram of BLDC-m with permanent magnets contains the PWM inverter, the current and

speed sensors and the controllers. An on-off controller with hysteresis is used in the inner current control loop; the phase selection block ensures the proper switching of the phases and the initialization as shown in [19]. A PI(D) controller is used in the main speed control loop. The cascade CS structure is presented in Fig. 4.2.8.

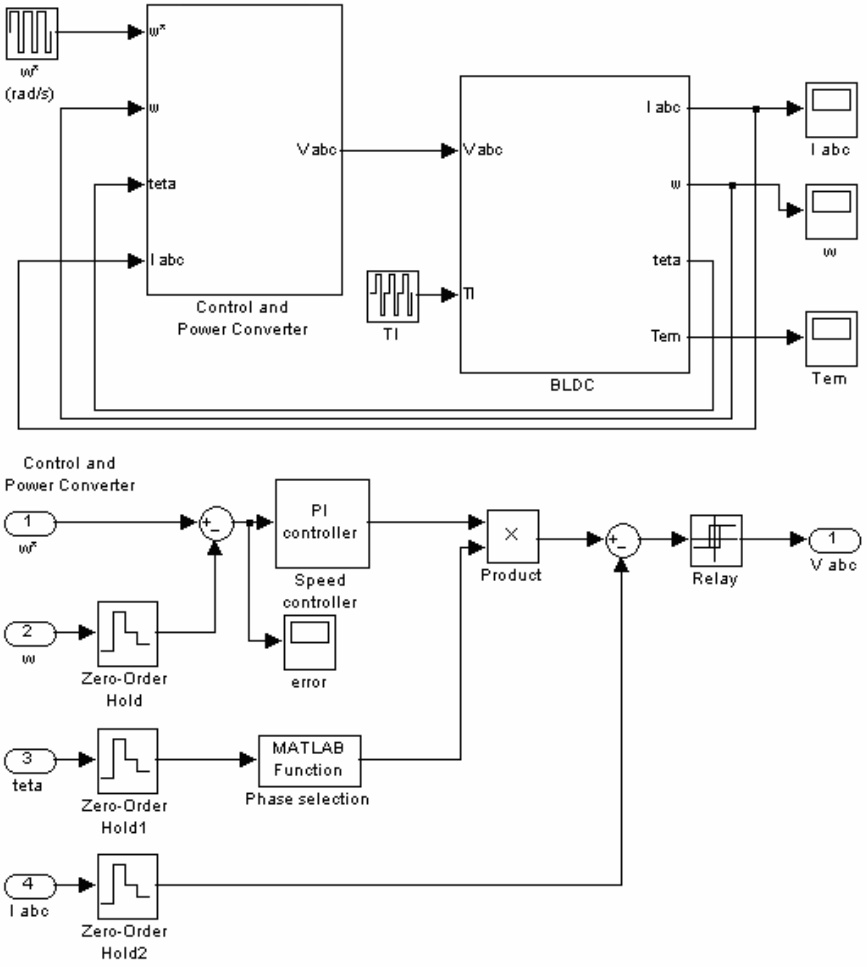

Fig. 4.2.8. Cascade control system structure for the process represented by the BLDC-m.

This application simulates a winding process with VMI and constant linear speed, $v_t(t) = \text{const}$ (Fig. 4.2.9), where the reference input is the linear speed of

the enrolled material which must be constant; so, the desired angular speed (ω) must be correlated with the modification of the working roll radius r_r; the controller parameters must be tuned and retuned as well.

To treat the first aspect, the following condition must be fulfilled:

$$v_t(t) = \text{const} \Rightarrow r(t) = k / r_r(t). \tag{4.2.38}$$

The measurement of $r_r(t)$ enables the continuous modification of the moment of inertia expressed as

$$J_e(t) = \frac{1}{2}\rho\,\pi\,l\,r_r^4(t). \tag{4.2.39}$$

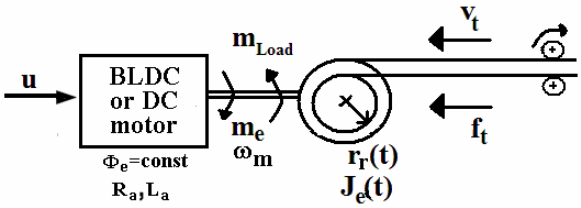

Fig. 4.2.9. Block diagram of the process in a VMI application.

The inner loop can be characterized generally by simplified benchmark-type second-order t.f.s connected to the operating point. The speed controller is of PI type, with an I component to ensure good tracking properties. The resulting open-loop t.f. with a double pole in the origin (imposed in the SO method)

$$H_0(s) = C(s)\cdot P(s) = \frac{k_0(1+sT_c)}{s^2(1+sT_\Sigma)}, \tag{4.2.40}$$

with $C(s) = H_C(s)$ and $P(s) = H_P(s)$, has $T_c = T_1 = T_m$ (the mechanical time constant which is time-variable and must be compensated), $k_0 = k_P k_c$, $T_1 >> T_\Sigma$. To ensure a desired phase margin, the open-loop gain k_0 must be maintained constant and the permanent recalculation of k_c according to (4.2.26) must be used (on the basis of the ESO-m).

A BLDC-m-based servo system with VMI characterized by the following parameters: p=2, R_a=1 Ω, L_a=0.02 H, V_{DC}= 220 V, J_{e0}= 0.005 kg m^2, is considered. The inner control loop ensures a second-order (with lag) process behavior characterized by (4.2.27) (a) with $k_P = 40$, $T_1 = 0.03$ s and $T_\Sigma = 0.015$ s. The

controlled parameters of BLDC-m, θ and *lpm*, were set to ensure that the motor can operate at any desired speed within $0 \le \omega \le 314\ s^{-1}$.

The tuning conditions (4.2.26) specific to the ESO method are applied setting the value $\beta = 12$ for the average value for $J_e(t)$, without parameter adaptation and ARW measure. The simulation scenario consists of a the starting regime (starting the BLDC motor, from 0 to 1 s), the constant reference for the linear speed (from 1 s to 1.5 s), the winding process starting (from 1.5 s to 3 s); the winding process stopping (from 3 *s* to 3.5 s) and the stopping regime for the BLDC-m, (from 3.5 s to 4.5 s). These regimes aim the modification of the angular speed ω to ensure the desired linear speed v_t accompanied by increasing $r_r(t)$ and $J_e(t)$ which require – according to (4.2.38) – the proper modification of the linear speed reference input $r(t)$. Figs. 4.2.10 to 4.2.14 synthesize a part of the simulation results.

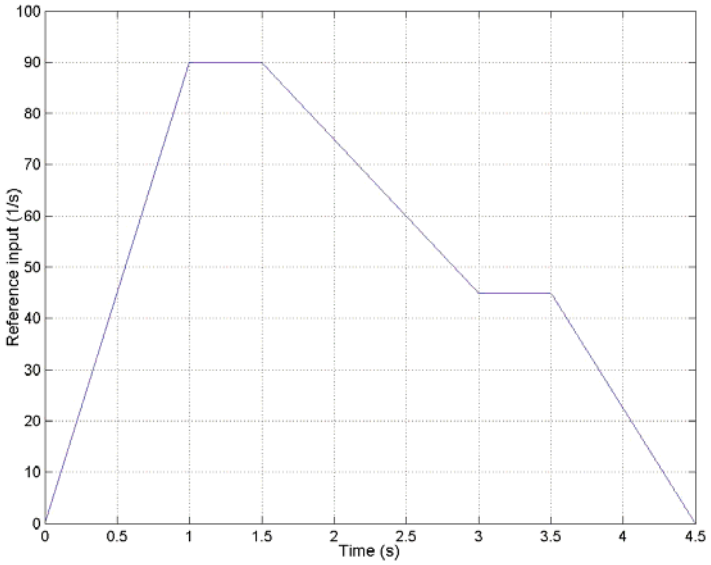

Fig. 4.2.10. Reference input versus time.

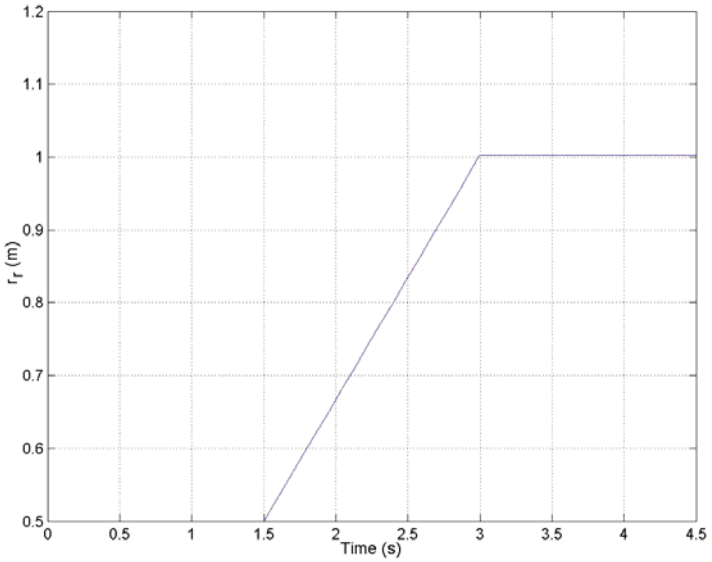

Fig. 4.2.11. Drum radius versus time.

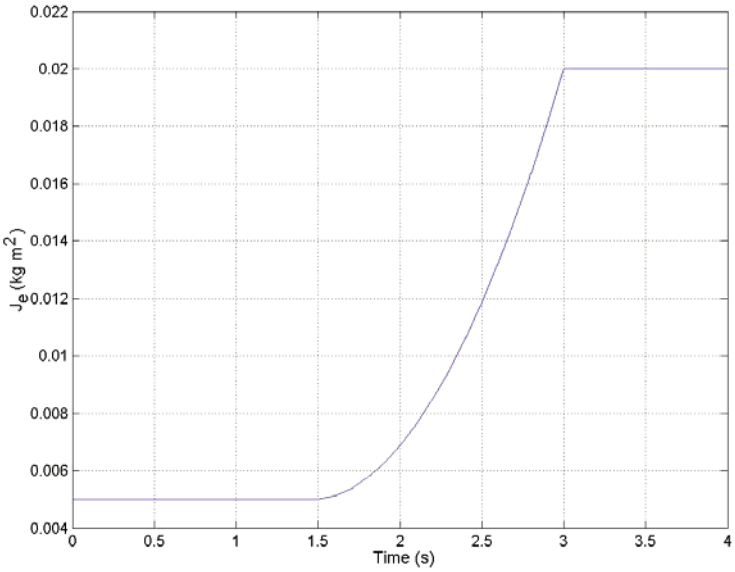

Fig. 4.2.12. Equivalent moment of inertia versus time.

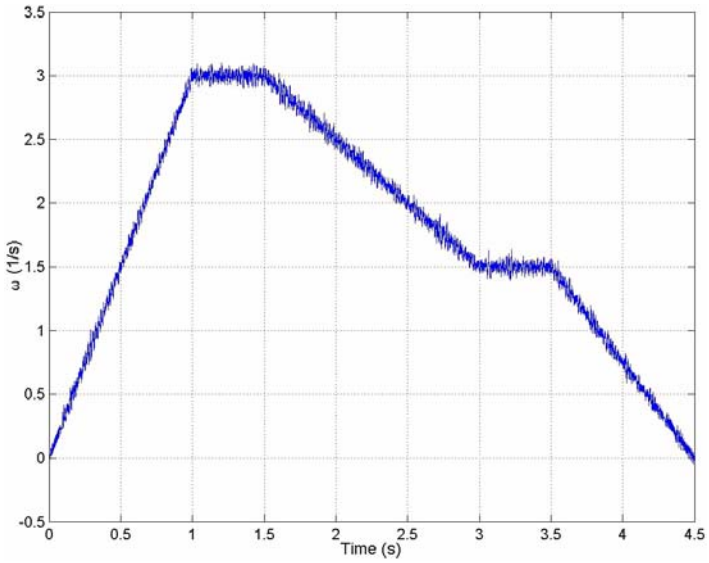

Fig. 4.2.13. Drum angular speed versus time.

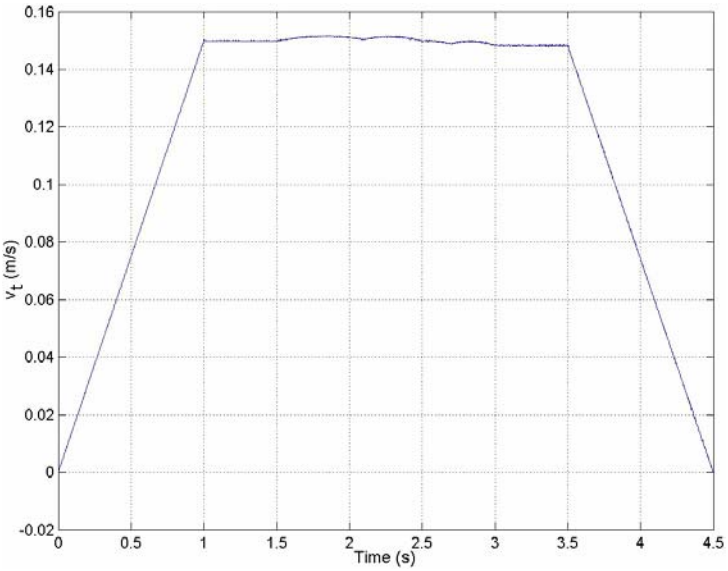

Fig. 4.2.14. Drum linear speed versus time.

References

[1] K. J. Åström and T. Hägglund, PID Controllers Theory: Design and Tuning, Instrument Society of America, Research Triangle Park, NC, 1995.

[2] A. O'Dwyer, "A summary of PI and PID controller tuning rules for processes with time delay, part I and part II", Preprints of IFAC Workshop on Digital Control: Past, Present and Future of PID control PID'00, Terrassa, Spain, pp. 175–180, 242–247, 2000.

[3] O. Föllinger, Regelungstechnik, Elitera Verlag, 1999.

[4] St. Preitl, R.-E. Precup, I.-B. Ursache, S. Gheju and Zs. Preitl, "Methodical aspects concerning the study of control solutions for plants with slow responses", Buletinul Stiintific al Universitatii "Politehnica" din Timisoara, Transactions on Automatic Control and Computer Science, vol. 49 (63), no. 1, pp. 127–132, 2004.

[5] J. Quevedo and T. Escobet (Eds.), Proceedings of IFAC Workshop on Digital Control: Past, Present and Future of PID control PID'00, Terrassa, Spain, Pergamon Press, 2000.

[6] R. Vilanova and A. Visioli (Eds.), Proceedings of 2nd IFAC Conference on Advances in PID Control PID'12, Brescia, Italy, Advances in PID Control, vol. 2, www.ifac-papersonline.net, 2012.

[7] St. Preitl and R.-E. Precup, "An extension of tuning relations after symmetrical optimum method for PI and PID controllers", Automatica, vol. 35, no. 10, pp. 1731–1736, 1999.

[8] Zs. Preitl, "PI and PID controller tuning method for a class of systems", Proceedings of SACCS 2001 Symposium, Iasi, Romania, 4 pp., 2001.

[9] Controlled air stream and temperature control plant LTR 701, Operating manual, Amira GmbH, Duisburg, Germany, 2002.

[10] C. Kessler, "Das symetrische Optimum", Regelungstechnik, vol. 6, pp. 395–400, 432–436, 1958.

[11] St. Preitl and R.-E. Precup, "Points of view in controller design by means of extended symmetrical optimum method," in: Control Systems Design 2003 (CSD '03), S. Kozak and M. Huba, Eds., Elsevier, pp. 95–100, 2004.

[12] J. Lehoczky, M. Márkus and S. Mucsi, Szervorendszerek követö szabályozások, MK, Budapest, 1977.

[13] L. Loron, "Tuning of PID controllers by the non-symmetrical optimum method", Automatica, vol. 33, no. 1, pp. 103–107, 1997.

[14] H. Lutz and W. Wendt, Taschenbuch der Regelungstechnik, Harri Deutsch Verlag, Frankfurt, 1998.

[15] Zs. Preitl, "Improving disturbance rejection by means of a double parameterization of the symmetrical optimum method", Scientific Bulletin of

the "Politehnica" University of Timisoara, Transactions on Automatic Control and Computer Science, vol. 50 (64), no. 1, pp. 25–34, 2005.

[16] Zs. Preitl, Model based design methods for speed control applications, Editura Politehnica, Timisoara, Romania, 2008.

[17] St. Preitl and R.-E. Precup, "Cross optimization aspects concerning the extended symmetrical optimum method", in: Digital Control 2000: Past, Present and Future of PID Control, J. Quevedo and T. Escobet, Eds., Elsevier Science, pp. 223–228, 2000.

[18] St. Preitl, A.-I. Stînean, R.-E. Precup, C.-A. Dragoş and M.-B. Rădac, "2-DOF and fuzzy control extensions of symmetrical optimum design method: Applications and perspectives", in: Applied Computational Intelligence in Engineering and Information Technology, R.-E. Precup, Sz. Kovács, St. Preitl and E. M. Petriu, Eds., Topics in Intelligent Engineering and Informatics, vol. 1, Springer-Verlag, pp. 19–37, 2012.

[19] St. Preitl, A.-I. Stînean, R.-E. Precup, Zs. Preitl, E. M. Petriu, C.-A. Dragoş and M.-B. Rădac, "Controller design methods for driving systems based on extensions of symmetrical optimum method with DC and BLDC motor applications", Proceedings of 2nd IFAC Conference on Advances in PID Control PID'12, Brescia, Italy, Advances in PID Control, vol. 2, R. Vilanova and A. Visioli, Eds., pp. 264–269, 2012.

[20] A.-I. Stînean, St. Preitl, R.-E. Precup, C.-A. Dragoş and M.-B. Rădac, "Classical and fuzzy approaches to 2-DOF control solutions for BLDC-m drives", in: Intelligent Systems: Models and Applications, E. Pap, Ed., Topics in Intelligent Engineering and Informatics, vol. 3, Springer-Verlag, pp. 175–193, 2013.

[21] A.-I. Stînean, St. Preitl, R.-E. Precup, C.-A. Dragoş, M.-B. Rădac and E. M. Petriu, "Modeling and control of an electric drive system with continuously variable reference, moment of inertia and load disturbance", Proceedings of 9th Asian Control Conference ASCC 2013, Istanbul, Turkey, paper 585, 6 pp., 2013.

[22] A.-I. Stînean, St. Preitl, R.-E. Precup, C.-A. Dragoş, M.-B. Rădac and E. M. Petriu, "Low-cost neuro-fuzzy control solution for servo systems with variable parameters", Proceedings of 2013 IEEE International Conference on Computational Intelligence and Virtual Environments for Measurement Systems and Applications CIVEMSA 2013, Milano, Italy, pp. 156–161, 2013.

[23] A.-I. Stînean, St. Preitl, R.-E. Precup, C.-A. Dragoş, E. M. Petriu and M.-B. Rădac, "Solutions to avoid the worst case scenario in driving systems working under continuously variable conditions", Proceedings of IEEE 9th International Conference on Computational Cybernetics ICCC 2013, Tihany, Hungary, pp. 339–344, 2013.

[24] St. Preitl, R.-E. Precup and Zs. Preitl, Process Control Structures and Algorithms, vols. 1 and 2 (in Romanian: Structuri si algoritmi pentru conducerea automata a proceselor), Editura Orizonturi Universitare Publishers, Timisoara, 2009.

[25] St. Preitl, R.-E. Precup, A.-I. Stînean, C.-A. Dragoş and M.-B. Rădac. "Extensions in symmetrical optimum design method. Advantages, applications and perspectives" Proceedings of 6th IEEE International Symposium on Applied Computational Intelligence and Informatics SACI 2011, Timisoara, Romania, pp. 17–22, 2012.

[26] M. Araki and H. Taguchi, "Two-degree-of-freedom PID controllers", International Journal of Control, Automation, and Systems, vol. 1, no. 4, pp. 401–411, 2003.

[27] S. A. Nasar and I. Boldea, I. Electric Drives, 2nd edition, CRC Press, Taylor & Francis, New York, 2005.